Diameter Controlled CVD Synthesis of Single-Walled Carbon Nanotubes

Theerapol Thurakitseree[1], Erik Einarsson[1,2], Rong Xiang[1,3], Pei Zhao[1], Shinya Aikawa[1], Shohei Chiashi[1], Junichiro Shiomi[1], and Shigeo Maruyama[1]*

Affiliation:

[1]Department of Mechanical Engineering, The University of Tokyo

[2]Global Center of Excellence for Mechanical Systems Innovation, The University of Tokyo

[3]HKUST-SYSU Joint Laboratory of Nano Materials and Technology, State Key Laboratory of Optoelectronic Materials and Technologies, School of Physics and Engineering, Sun Yat-Sen University

Mailing Address:

[1]Department of Mechanical Engineering, The University of Tokyo, 7-3-1 Hongo, Bunkyo-ku, Tokyo 113-8656, Japan

[2]Global Center of Excellence for Mechanical Systems Innovation, The University of Tokyo, 7-3-1 Hongo, Bunkyo-ku, Tokyo 113-8656, Japan

[3]HKUST-SYSU Joint Laboratory of Nano Materials and Technology, State Key Laboratory of Optoelectronic Materials and Technologies, School of Physics and Engineering, Sun Yat-Sen University, Guangzhou 510275, China

Phone: +81-3-5841-6421

Fax: +81-3-5800-6983

E-mail: maruyama@photon.t.u-tokyo.ac.jp

Submitted: November 10, 2010

Accepted: February 1, 2011

Email address: maruyama@photon.t.u-tokyo.ac.jp

Abstract

In this study, we systematically investigated the influence of catalyst preparation procedures on the mean diameter of single-walled carbon nanotubes (SWNTs) synthesized by the alcohol catalytic chemical vapor deposition (ACCVD) process. It was found that the SWNT diameter is dependent upon both reduction temperature and time, with lower reduction temperature and/or shorter reduction time resulting in smaller diameter SWNTs. The morphology of the SWNTs also changed from vertically aligned to randomly oriented when the reduction temperature was below 500˚C. We also found that introducing a small amount of water during the catalyst reduction stage significantly decreased the mean diameter of the SWNTs. Lastly, we report on the use of a new binary catalyst system in which rhodium was combined with cobalt. This new Co/Rh combination produced SWNTs of smaller diameter than the conventional Co/Mo catalyst.

Keywords: Single-walled carbon nanotube, Alcohol, Chemical vapor deposition, Catalyst pretreatment, Rhodium co-catalyst

1. INTRODUCTION

Single-walled carbon nanotubes (SWNTs) have been the focus of considerable research because of their outstanding physical properties. Many of these properties, however, are heterogeneous in bulk samples because they are dependent on the diameter or structure of each SWNT. Thus, synthesis of SWNTs with nearly uniform diameters is required for some applications such as electrical circuits[1-3], optical devices[4,5], and solar cells[6-8]. Many groups are already working on producing small-diameter SWNTs, and many methods have been reported to control or reduce the SWNT diameter. Some of these methods include using various supporting materials[9-11], changing the catalyst composition[12], and changing pre-CVD treatment conditions[13].

During the CVD process, catalyst reduction is one step that influences the catalyst nanoparticle size. In this study, we investigated the influence of the catalyst reduction temperature and time on the average diameter of synthesized SWNTs synthesized by the alcohol catalytic CVD (ACCVD) process[14,15]. Additionally, following the report by Hata *et al.*[16] water-assisted CVD has been widely used to obtain high-yield growth of vertically aligned carbon nanotubes, but its role in catalyst reduction has remained largely unstudied. Here we also investigated the influence of water on catalyst reduction, and found the average SWNT diameter was significantly reduced by water-assisted reduction.

Lastly, many metals have been used as active catalysts for SWNT growth under various conditions[17,18], yet much of this vast parameter space remains unexplored. Here we explore the use of rhodium (Rh) as a catalyst for SWNT synthesis, and present Co/Rh as a new type of binary catalyst system for synthesis of small-diameter SWNTs.

2. EXPERIMENTAL SECTION

SWNTs were synthesized on silicon substrates (50 nm oxide layer) and quartz substrates by the ACCVD method. The influence of synthesis parameters on the average SWNT diameter was thoroughly evaluated using resonance Raman spectroscopy, optical absorbance spectroscopy, scanning electron microscopy (SEM), transmission electron microscope (TEM), photoluminescence excitation spectroscopy (PLE), and thermogravimetric analysis (TGA).

Cobalt and molybdenum binary catalysts were deposited by dip-coating[19] into a precursor solution containing 0.01 %wt of each metal species. The reduction process was modified to reduce the Co/Mo binary system at different temperatures—ranging from 300 to 800˚C—by flowing Ar containing 3% H_2 (Ar/H_2) at a flow rate of 300 sccm and a pressure of 60 kPa. The different heating and reduction stages are shown in Figure 1(a). Following this reduction, SWNTs were synthesized by flowing 450 sccm of ethanol at a pressure of 1.3 kPa for 5 min at a growth temperature of 800°C. The results from this reduction process were compared to the case of continuous reduction (our standard method), in which Ar/H_2 is present at a pressure of 40 kPa and a flow rate of 350 sccm throughout the heating process. Furthermore, the time-dependence of constant-temperature reduction was also investigated (Fig. 1b), where SWNTs were synthesized after reduction at 700˚C for 5, 30 and 100 min.

The influence of water on catalyst reduction was investigated by introducing a small amount (100 μL) of distilled water into the CVD system in addition to the Ar/H_2 typically used for reduction. The water was measured by micropipette and placed into the cap of a valve located upstream of the furnace. After evacuating the CVD chamber

to a base pressure below 15 Pa, the downstream valves were sealed and the water was introduced into the chamber. The vapor pressure of the water reached approximately 2.5 kPa. Following the introduction of water, Ar/H_2 was also introduced into the CVD chamber until the total pressure reached approximately 40 kPa. These gases remained in the CVD chamber for approximately 30 minutes while heating to the growth temperature of 800˚C. Upon reaching 800˚C, both water and Ar/H_2 were evacuated from the CVD chamber before introducing ethanol.

Lastly, a new noble transition metal was used in the binary catalyst. Rhodium(II) acetate, $C_8H_{16}O_{10}Rh_2$ (Wako, dimer dehydrate grade) dissolved in ethanol with a Rh concentration of 0.01 %wt, was used in place of molybdenum in the dip-coating process. After dip-coating both Rh and Co, the catalyst was reduced as per standard procedure under a continuous Ar/H_2 supply during heating to 800˚C. After reaching 800˚C, SWNTs were synthesized by introducing ethanol for 10 min at 1.3 kPa and a flow rate of 450 sccm. Resonance Raman spectra and SEM micrographs of the resulting SWNTs were compared with those obtained from SWNTs synthesized using our standard Co/Mo system.

USY-zeolite powder was also employed to support Co/Fe, Co/Mo and Co/Rh binary catalysts. In this case, the catalyst was prepared using the impregnation method according to previously reported procedures[20,21]. The concentrations of each metal were 2.5 %wt, and SWNTs grown from these catalytic powders were compared with HiPco SWNTs[22] based on characterization by resonance Raman spectroscopy, UV-vis-NIR absorbance spectroscopy, and photoluminescence excitation (PLE) spectroscopy. To obtain absorption and PLE spectra, as-grown SWNTs were dispersed in 2 mL of D_2O containing 0.1 g of sodium deoxycholate (DOC) by bath sonication for 1 h and an

additional 20 min of ultrasonication (Hielscher Ultrasonics GmbH UP400S with H3/Micro Tip 3 at a power flux level of 400 W cm^{-2}). This suspension was then centrifuged for 30 min at 8500 rpm (6623 g) and the supernatant was extracted for measurement.

3. RESULTS AND DISCUSSION

3.1. Effect of temperature and time for catalyst reduction on SWNT structures

Continuous Ar/H_2 reduction while heating the CVD chamber to the growth temperature has been our standard method for the synthesis of vertically aligned SWNTs. However, we expect the process might be improved by performing the catalyst reduction step at a fixed temperature, thus eliminating any dependence on the heating rate. Figure 2(a) compares the radial breathing mode (RBM) regions of resonance Raman spectra of SWNTs synthesized after reduction by Ar/H_2 at a constant heating rate and after reduction at different fixed temperatures. For excitation with 488 nm light, the spectra are characteristic[23] of vertically aligned SWNTs, particularly the dominant peak at 180 cm^{-1}. SEM observation [Figure 2(b)] revealed that SWNTs synthesized after reduction at temperatures lower than 500˚C were randomly aligned. This indicates that low-temperature reduction is too mild to reach the minimum areal density of active catalyst particles necessary to achieve vertical alignment. The RBM specrta in Figure 2(a), however, indicate a decrease in the SWNT diameters for lower reduction temperatures. We believe this is due to reduced diffusion and agglomeration of catalysts particles at lower reduction temperatures. Evidence for smaller diameters was also

evident from UV-vis-NIR absorbance spectra, shown in Figure 3. These absorbance spectra show the region of the first optical band gap (E_{11}), which can be used to estimate the mean SWNT diameter[24]. A slight blue-shift of the E_{11} of SWNTs synthesized after reduction at lower temperature indicates a smaller average SWNT diameter.

We also investigated the influence of reduction time on the diameter and morphology of SWNTs. Resonance Raman spectra of SWNTs grown after different catalyst reduction times at a fixed temperature showed little difference. However, UV-vis-NIR spectra indicate the average diameter of the SWNTs increased slightly after extended reduction at a given temperature (not shown). The final SWNT film thickness was also found to be reduced after extended reduction time.

3.2. Water-assisted pretreatment of catalysts

CVD has become the most widely used method for SWNT synthesis, and the presence of water during CVD has been shown to considerably affect the synthesis[16] of SWNTs. However, water is typically introduced together with the carbon source in order to extend the catalyst lifetime[16,25]. This has also been shown to inhibit Ostwald ripening of the catalyst particles during CVD[26]. By employing ethanol as a carbon feedstock, introduction of additional water is unnecessary since it is produced from thermal decomposition of ethanol at the growth temperature[12,27]. However, Bezemer *et al.* have reported[28] that the size and diameter distribution of Co catalyst particles can be reduced by exposure to a combination of H_2O, H_2, and Ar. Based on this report, we investigated the effect of H_2O on catalyst preparation, i.e., reduction of catalyst prior to introduction of the carbon feedstock.

Figure 4(a) shows SEM images of SWNTs grown on quartz substrates with and without water-assisted reduction. The images clearly show the morphology changes from vertical to random orientation after water-assisted reduction, and the SWNT yield is considerably lower. However, resonance Raman spectra and optical absorbance spectra indicate a significant decrease in SWNT diameter. In Figure 4(b), the intensity of the small-diameter peaks around 200 and 250 cm^{-1} (for 488 nm excitation) are clearly stronger than for SWNTs grown by our standard procedure. Additionally, the strong Breit-Wigner-Fano (BWF) feature in the G-band region also indicates an increase in the population of small-diameter metallic SWNTs for the water-assisted reduction case. Similar trends can also be clearly seen from the Raman spectra obtained using other excitation wavelengths (514 and 633 nm). Furthermore, optical absorbance spectra (Figure 5) clearly show a significant difference in the mean SWNT diameter. The position of the E_{11} peak was shifted from a position near 2400 nm (approx. 0.5 eV) up to ~1200 nm (approx. 1.0 eV). This corresponds to a change in average diameter from 1.9 nm to 1.0 nm. In the latter case, the E_{22} feature is visible near 750 nm, indicating our assignment of the E_{11} peak at 1200 nm is correct.

A previous study[29] on our Co/Mo dip-coated catalyst revealed the state of the catalyst prior to reduction to be Co and Mo oxides. The influence of water on this system may be explained by the findings of Bezemer *et al.*[28], i.e., that the combined presence of Ar, H_2, and H_2O strongly suppresses Co particle growth at high temperature. We suspect the production of OH radicals during the heating process[30], in which surface hydroxyls are produced from the reaction between water and metal oxide (*O*), i.e., $H_2O + *O* \leftrightarrow 2OH*$. This state, shown in Figure 6, could be responsible for inhibiting both catalyst aggregation and reduction. Additionally, Alcanter *et al.*[31] reported that

various metals and metal oxides–including silicon and silicon dioxide–can achieve high surface concentrations of hydroxyl groups after exposure to H_2O/O_2 in high energy environments such as steam (1050 °C) and water plasma. This supports the findings of Bezemer *et al.*[28] and indicates surface hydroxyls would be stable at catalyst reduction and SWNT synthesis temperatures.

3.3. New binary catalyst combination

Rhodium, which is a noble metal and in the same group as Co, has been used to catalyze SWNT growth by pulsed laser vaporization[32]. However, it has not been well incorporated into a binary catalyst system even though it has been shown to stabilize metal acetates[33]. The advantage of using binary catalyst systems has been known for some time, and in a previous study we have shown that in the Co/Mo binary system, Mo helps prevent agglomeration of Co at high temperatures before and during CVD[34]. Similarly, the addition of Rh to Co/SiO_2 has also been reported to increase reducibility of catalysts with a small crystalline size[35]. Based on this knowledge, we incorporated Rh into a binary catalyst system in order to stabilize Co and reduce the diameter of resulting SWNTs.

Figure 7 shows resonance Raman spectra of SWNTs grown from Co/Rh and Co/Mo binary catalysts obtained using different excitation wavelengths (488, 514 and 633 nm). The shift in spectral weight toward higher energy indicates the SWNT diameters are smaller in the Co/Rh binary system. This can be explained by the aforementioned strong interaction between Rh and Co, which should keep the nanoparticle diameter small and has been shown to result in increased magnetization[36]

for Co/Rh. The yield of SWNTs, however, was much lower than from Co/Mo because the growth-stage energetics are more favorable[37] for Mo than for Rh. We also speculate that the formation of a CoRh alloy may be at least partially responsible for the low yield.

In an attempt to improve both the yield and diameter selectivity of the Co/Rh catalysts, USY-zeolite was used as a supporting material. On zeolite, Co/Fe binary catalysts produced the highest yield, even though the SWNT diameter is similar to the case of Co/Rh, whereas Co/Mo on zeolite produced the lowest yield. Resonance Raman spectra [Figures 8(a) – 8(c)] of as-grown SWNTs synthesized from different catalytic powders indicate that SWNTs grown from Co/Mo binary catalysts have larger diameters, whereas Co/Rh and Co/Fe catalyst systems produce small-diameter SWNTs. In addition, the similarity in diameters between SWNTs synthesized from Co/Fe and Co/Rh was also confirmed by UV-vis-NIR absorbance spectra, shown in Figure 8(d). These results are consistent with resonance Raman spectra, but absorbance peaks of SWNTs grown from Co/Mo catalyst were somewhat downshifted in energy.

Figure 9 shows photoluminescence excitation (PLE) maps of dispersed SWNTs grown from various catalyst powders, and of HiPco SWNTs for comparison. Absorbance spectra shown in Figure 8 were obtained using the same samples. The fluorescence emission wavelength range was recorded from 900 to 1400 nm, while the excitation wavelength was scanned from 500 to 850 nm in 5 nm steps. Each peak in the PLE map[38] corresponds to emission from the first optical band gap (E_{11}) of semiconducting SWNTs that had been excited at the second optical band gap (E_{22}). These PLE maps show that Co/Fe and Co/Rh binary catalysts produce SWNTs with similar diameters, both of which are smaller than HiPco SWNTs. The tendency for

Co/Mo catalyst to produce SWNTs with a larger average diameter is in agreement with optical absorbance and resonance Raman spectra, however PLE spectra indicate that SWNTs synthesized from Co/Mo catalyst on zeolite have a narrower diameter distribution than others, including HiPco SWNTs. In addition, the presence of SWNTs in all of these samples was confirmed by TEM observation (not shown), and the average diameters were determined to be approximately 1 nm in the case of Co/Rh and Co/Fe, and 1.4 nm in the case of Co/Mo.

By considering the possible mechanism of these three catalyst treatment procedures, it is possible that either catalyst reduction and/or the use of Rh as a Co supporting material reduces the number of active Co catalyst particles. This would reduce the areal density of active catalyst, causing less aggregation and resulting in the synthesis of SWNTs with smaller diameters but in lower yield. These results are also in agreement with our previous study[12], where we showed that reducing the concentration of Co produces SWNTs with smaller diameters and lower yield. Despite the similar trend, however, the average diameter of SWNTs synthesized after water-assisted reduction reported here is considerably smaller than obtained in our prior study.

4. CONCLUSION

We investigated the influence of various catalyst preparation parameters on the average diameter of SWNTs synthesized by the ACCVD method. We found the average diameter to be dependent on the catalyst reduction temperature and time, with smaller diameter SWNTs obtained by reduction at low temperature and/or for a short time. However, low-temperature reduction resulted in low yield and random orientation

instead of vertical alignment. Introducing water into the Ar/H_2 atmosphere during the reduction stage significantly reduced the average SWNT diameter. We also report the synthesis of small-diameter SWNTs using a new Co/Rh binary catalyst. SWNTs synthesized from Co/Rh had diameters similar to those synthesized from Co/Fe (mean diameter approximately 1 nm), and smaller than HiPco SWNTs.

Acknowledgements

Part of this work was financially supported by Grants-in-Aid for Scientific Research (19054003 and 22246023), NEDO (Japan), "Development of Nanoelectronic Device Technology" of NEDO, and the Global COE Program "Global Center for Excellence for Mechanical Systems Innovation". TT acknowledges a scholarship granted by the Office of the Higher Education Commission, Thailand.

References

1. S. J. Kang, C. Kobacas, T. Ozel, M. Shim, N. Pimparkar, M. A. Alam, S. V. Rotkin, and J. A. Rogers, *Nature Nanotech.* 2, 230 **(2007)**.
2. C. Kobacas, N. Pimparkar, O. Yesilyurt, S. J. Kang, M. A. Alam, and J. A. Rogers, *Nano Lett.* 7, 1195 **(2007)**.
3. Q. Cao, H. S. Kim, N. Pimparkar, J. P. Kulkarni, C. Wang, M. Shim, K. Roy, M. A. Alam, and J. A. Rogers, *Nature* 454, 495 **(2008)**.
4. N. M. Gabor, Z. Zhong, K. Bosnick, J. Park, and P. L. McEuen, *Science* 325, 1367

(2009).

5. S. Kivisto, T. Hakulinen, A. Kaskela, B. Aitchison, D. P. Borwn, A. G. Nasibulin, E. L. Kauppinen, A. Harkonen, and O. G. Okhotnikov, *Optics Express* 17, 2358 **(2009)**.
6. T. Umeyama and H. Imahori, *Energy Environ. Sci.* 1, 120 **(2008)**.
7. H. Li, W. K. Loke, Q. Zhang, and S. F. Yoon, *Appl. Phys. Lett.* 96, 043501 **(2010)**.
8. D. J. Bindl, M. Y. Wu, F. C. Prehn, and M. S. Arnold, *Nano Lett.* DOI: 10.1021/nl1031343 (2010).
9. B. Kitiyanan, W. E. Alvarez, J. H. Harwell, and D. E. Resasco, *Chem. Phys. Lett.* 317, 497 **(2000)**.
10. B. Wang, Y. Yang, L. J. Li, and Y. Chen, *J. Mater. Sci.* 44, 3285 **(2009)**.
11. H. Sugime and S. Noda, *Carbon* 48, 2203 **(2010)**.
12. R. Xiang, E. Einarsson, J. Okawa, T. Thurakitseree, Y. Murakami, J. Shiomi, Y. Ohno, and S. Maruyama, *J. Nanosci. Nanotechnol.* 10, 3901 **(2010)**.
13. A. R. Harutyunyan, G. Chen, T. M. Paronyan, E. M. Pigos, O. A. Kuznetsov, K. Hewaparakrama, S. M. Kim, D. Zakharov, E. A. Stach, and G. U. Sumanasekera, *Science*, 236, 116 **(2009)**.
14. S. Maruyama, R. Kojima, Y. Miyauchi, S. Chiashi, and M. Kohno, *Chem. Phys. Lett.* 360, 229 **(2002)**.
15. Y. Murakami, S. Chiashi, Y. Miyauchi, M. Hu, M. Ogura, T. Okubo, and S. Maruyama, *Chem. Phys. Lett.* 385, 298 **(2004)**.
16. K. Hata, D. N. Futaba, K. Mizuno, T. Namai, M. Yumura, and S. Iijima, *Science* 306, 1362 **(2004)**.
17. D. Takagi, Y. Homma, H. Hibino, S. Suzuki, and Y. Kobayashi, *Nano Lett.* 6, 2642

(2006).

18. D. Yuan, L. Ding, H. Chu, Y. Feng, T. P. McNicholas, and J. Liu, *Nano Lett.* 8, 2576 **(2008)**.
19. Y. Murakami, Y. Miyauchi, S. Chiashi, and S. Maruyama, *Chem. Phys. Lett.* 377, 49 **(2003)**.
20. S. Maruyama, R. Kojima, Y. Miyauchi, S. Chiashi, and M. Kohno, *Chem. Phys. Lett.* 360, 229 **(2002)**.
21. Y. Murakami, Y. Miyauchi, S. Chiashi, and S. Maruyama, *Chem. Phys. Lett.* 374, 53 **(2003)**.
22. P. Nikolaev, M. J. Bronikowski, R. K. Bradley, F. Rohmund, D. T. Colbert, K. A. Smith, and R. E. Smalley, *Chem. Phys. Lett.* 313, 91 **(1999)**.
23. Y. Murakami, S. Chiashi, E. Einarsson, and S. Maruyama, *Phys. Rev. B.* 71, 085403 **(2005)**.
24. H. Kataura, Y. Kumazawa, Y. Maniwa, I. Umezu, S. Suzuki, Y. Ohtsuka, Y. Achiba, *Synth. Met.* 103, 2555 **(1999)**.
25. D. N. Futaba, K. Hata, T. Namai, T. Yamada, K. Mizuno, Y. Hayamizu, M. Yumura, and S. Iijima, *J. Phys. Chem. B* 110, 8035 **(2006)**.
26. P. B. Amama, C. L. Pint, L. McJilton, S. M. Kim, E. A. Stach, P. T. Murray, R. H. Hauge, and B. Maruyama, *Nano Lett.* 9, 44 **(2009)**.
27. H. Sugime, S. Noda, S. Maruyama, and Y. Yamaguchi, *Carbon* 47, 234 **(2009)**.
28. G. L. Bezemer, T. J. Remans, A. P. van Bavel, and A. I. Dugulan, *J. Am. Chem. Soc.* 132, 8540 **(2010)**.
29. M. H. Hu, Y. Murakami, M. Ogura, S. Maruyama, and T. Okubo, *J. Catalysis* 225, 230 **(2004)**.

30. R. Hakkarainen and T. Salmi, *Appl. Catalyst A* 99, 195 **(1993)**.
31. N. A. Alcantar, E. S. Aydil, and J. N. Israelachvili, in *Fundamental & Applied Aspects of Chemically Modified Surfaces*, edited J. P. Blitz, C. B. Little, Roy. Soc. Chem. **(1999)**, p. 212.
32. P. Nikolaev, W. Holmes, E. Sosa, P. Boul, S. Arepalli, and L. Yowell, *J. Nanosci. Nanotechnol.* 10, 3780 **(2010)**.
33. M. Bowker, and T. J. Cassidy, *J. Catalysis* 174, 65 **(1998)**.
34. W. E. Alvarez, B. Kitiyanan, A. Borgna, and D. E. Resasco, *Carbon* 39, 547 **(2001)**.
35. B. P. Evandro, H. Narcis, M. Salvador, J. L. G. Fierro, and P. Ramirez de la Piscina, *J. Catalysis* 257, 206 **(2008)**.
36. J. W. A. Robinson, Z. H. Barber, and M. G. Blamire, *Appl. Phys. Lett.* 95, 192509 **(2009)**.
37. W. Q. Deng, X. Xu, and W. A. Goddard, *Nano Lett.* 4, 2331 **(2004)**.
38. M. J. O'Connell, S. M. Bachilo, C. B. Huffman, V. C. Moore, M. S. Strano, E. H. Haroz, K. L. Rialon, P. J. Boul, W. H. Noon, C. Kittrell, J. Ma, R. H. Hauge, R. B. Weisman, and R. E. Smalley, *Science* 297, 593 **(2002)**.

Figure Captions

Figure 1. (a) Temperature profiles of different catalyst reduction processes; black, solid red, and dashed red lines represent heating, Ar/H_2 reduction at a constant temperature, and continuous Ar/H_2 reduction, respectively; (b) catalyst reduction at 700 °C for different times (5, 30, and 100 min).

Figure 2. (a) Resonance Raman spectra of as-grown SWNTs for each reduction condition compared with the case of continuous reduction; (b) SEM images of SWNTs grown after different constant-temperature reduction conditions.

Figure 3. Absorbance spectra of as-grown SWNTs synthesized after reduction at different temperatures.

Figure 4. (a) SEM images showing the change in morphology and (b) resonance Raman spectra indicating the smaller diameters of SWNTs grown from Co/Mo catalysts treated with H_2O.

Figure 5. Normalized optical absorption spectra of as-grown SWNTs synthesized from Co/Mo catalysts treated with and without H_2O clearly show a blueshift in the E_{11} peak position, indicating a significant decrease in mean SWNT diameter.

Figure 6. Model of the surface hydroxyl formed from the reaction between water and substrate-supported binary catalyst.

Figure 7. Resonance Raman spectra of SWNTs grown from the Co/Rh binary system (thick solid line) compared with those grown from the Co/Mo binary system (thin solid line). Excitation laser wavelengths (in nm) are indicated next to the spectra, and the colors correspond approximately to the color of the excitation laser.

Figure 8. (a) – (c) Resonance Raman spectra and (d) optical absorbance spectra of SWNTs grown from different catalytic powders. Resonance Raman excitation

wavelengths are indicated.

Figure 9. Comparison of photoluminescence excitation (PLE) maps for SWNTs grown from three different binary catalyst systems and HiPco SWNTs.

Figure 1.

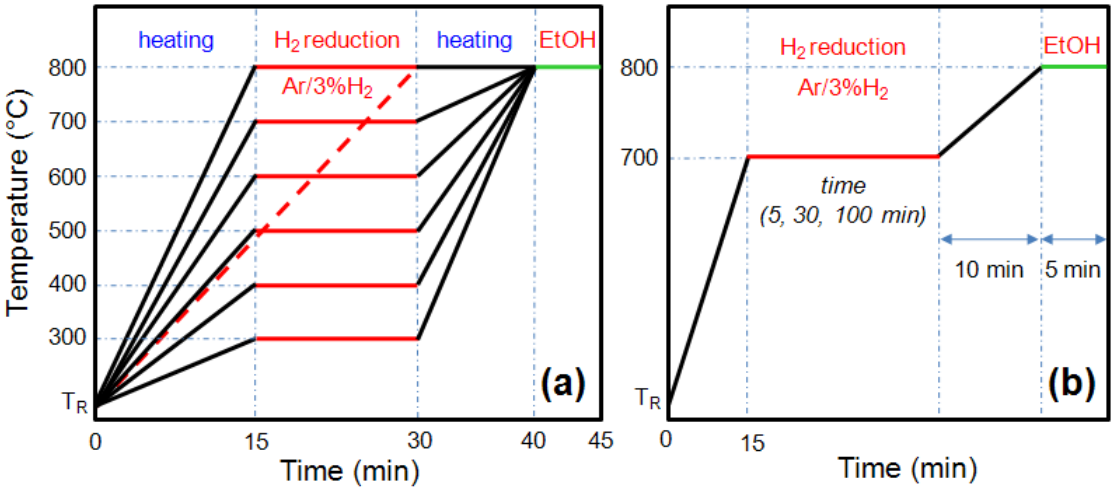
heating
H2 reduction
heating
EtOH
Ar/3%H2
Temperature (°C)
800
700
600
500
400
300
TR
0
15
30
40
45
Time (min)
(a)
H2 reduction
EtOH
Ar/3%H2
800
700
time
(5, 30, 100 min)
10 min
5 min
TR
0
15
Time (min)
(b)

Figure 2.

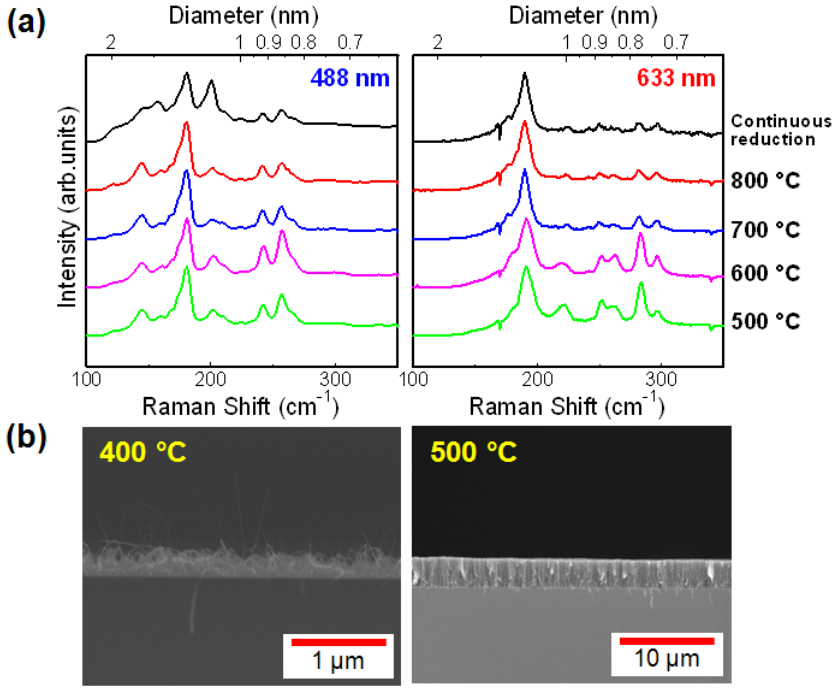
(a)
Diameter (nm)
2
1
0.9
0.8
0.7
488 nm
633 nm
Intensity (arb.units)
Continuous reduction
800 °C
700 °C
600 °C
500 °C
100
200
300
Raman Shift (cm-1)
(b)
400 °C
500 °C
1 μm
10 μm

Figure 3.

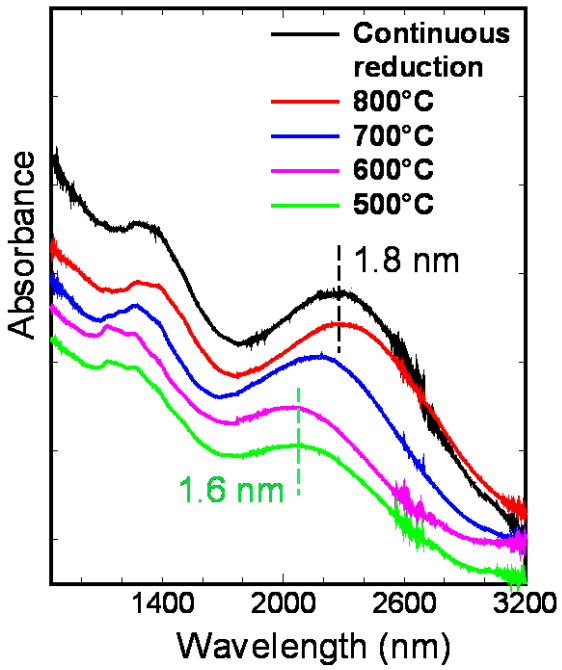
Continuous reduction
800°C
700°C
600°C
500°C
1.8 nm
1.6 nm
Absorbance
1400
2000
2600
3200
Wavelength (nm)

Figure 4.

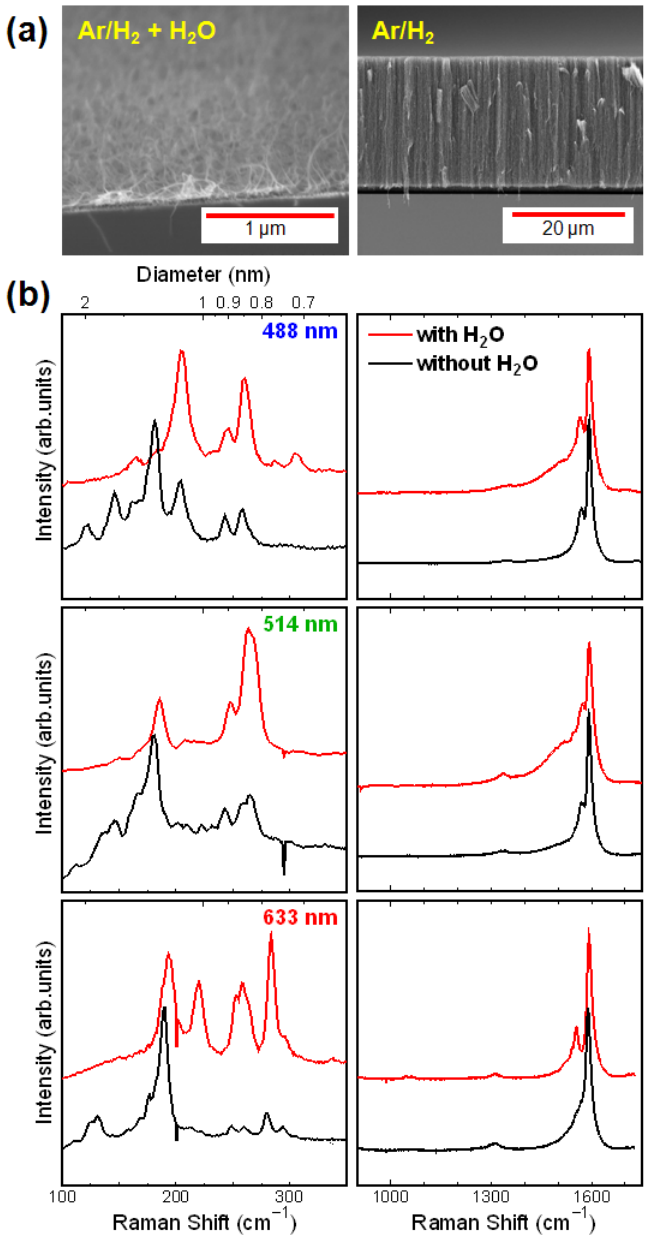
(a)
Ar/H2 + H2O
Ar/H2
1 μm
20 μm
(b)
Diameter (nm)
2
1
0.9
0.8
0.7
488 nm
514 nm
633 nm
with H2O
without H2O
Intensity (arb.units)
100
200
300
1000
1300
1600
Raman Shift (cm−1)

Figure 5.

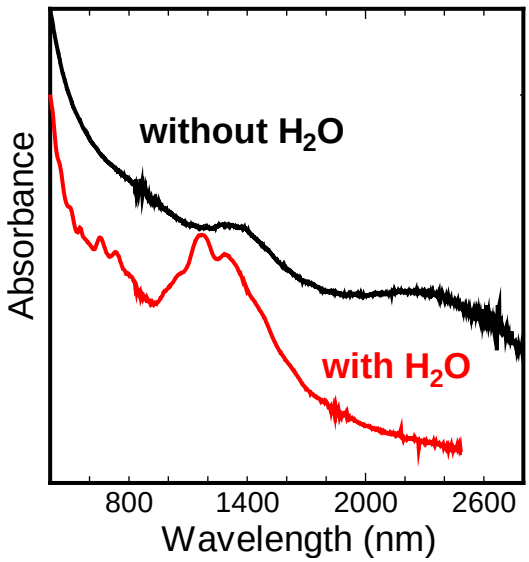
without H_2O
with H_2O
Absorbance
800
1400
2000
2600
Wavelength (nm)

Figure 6.

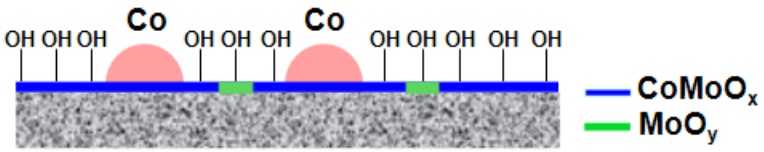

Figure 7.

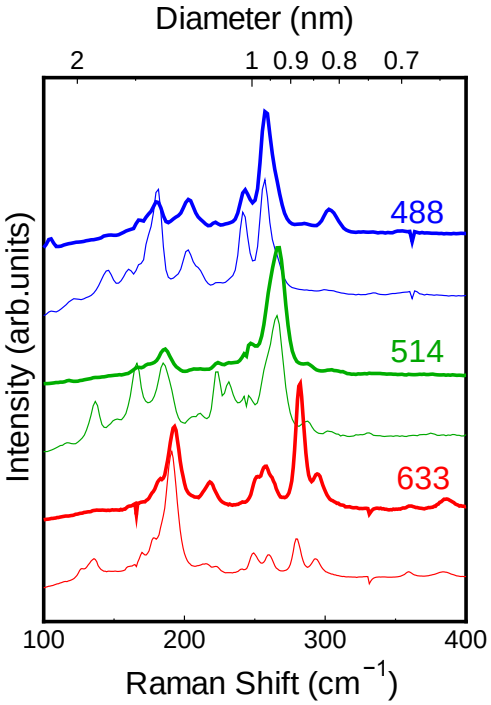
Diameter (nm)
2
1
0.9
0.8
0.7
488
514
633
Intensity (arb.units)
100
200
300
400
Raman Shift (cm^{-1})

Figure 8.

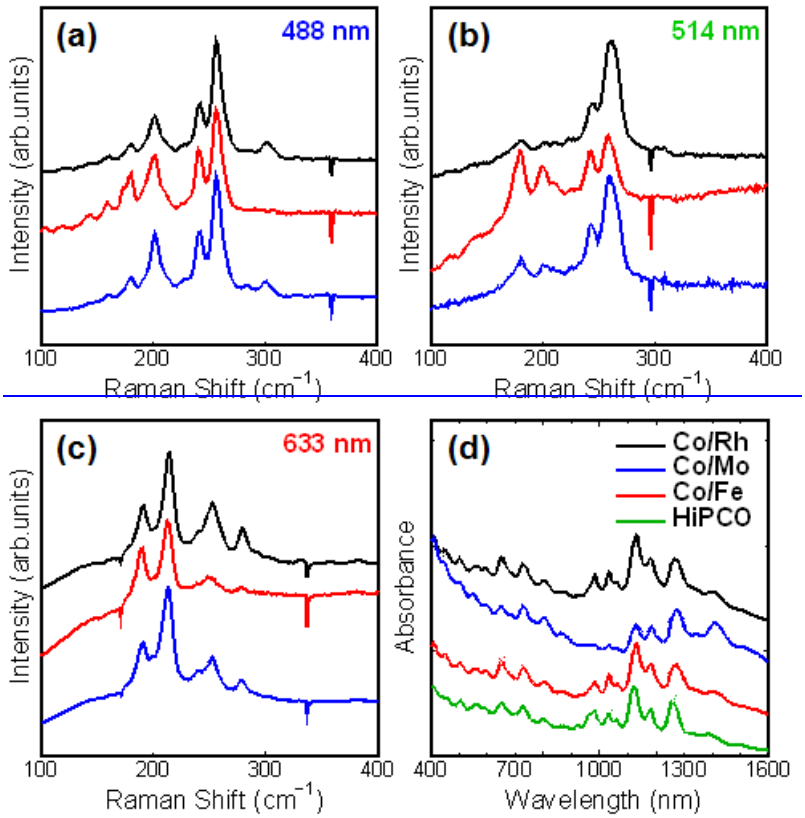
(a)
488 nm
Intensity (arb.units)
100
200
300
400
Raman Shift (cm^{-1})
(b)
514 nm
Intensity (arb.units)
100
200
300
400
Raman Shift (cm^{-1})
(c)
633 nm
Intensity (arb.units)
100
200
300
400
Raman Shift (cm^{-1})
(d)
Co/Rh
Co/Mo
Co/Fe
HiPCO
Absorbance
400
700
1000
1300
1600
Wavelength (nm)

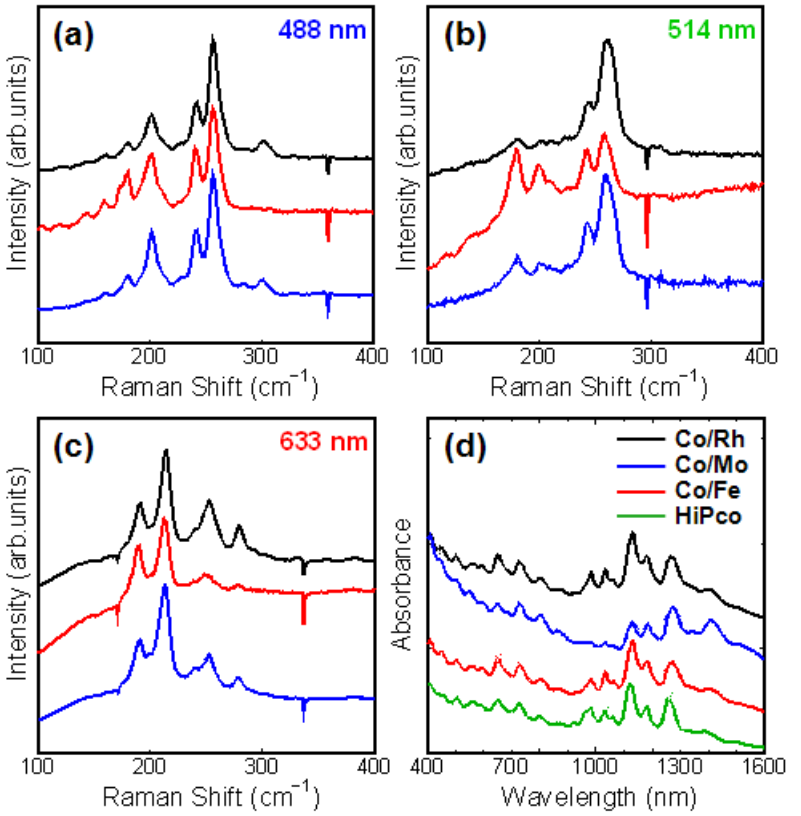
(a)
488 nm
Intensity (arb.units)
Raman Shift (cm^{-1})
(b)
514 nm
Intensity (arb.units)
Raman Shift (cm^{-1})
(c)
633 nm
Intensity (arb.units)
Raman Shift (cm^{-1})
(d)
Co/Rh
Co/Mo
Co/Fe
HiPco
Absorbance
Wavelength (nm)

Figure 9.

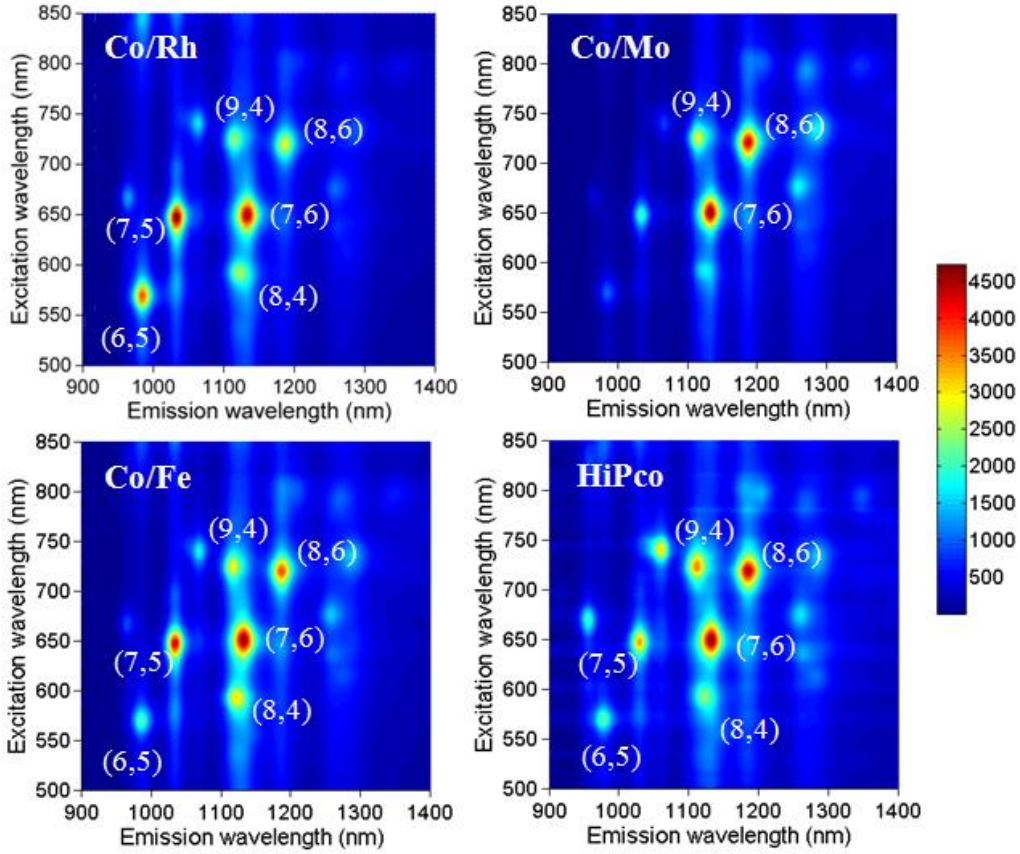
Co/Rh
(9,4)
(8,6)
(7,5)
(7,6)
(8,4)
(6,5)
Co/Mo
(9,4)
(8,6)
(7,6)
Co/Fe
(9,4)
(8,6)
(7,5)
(7,6)
(8,4)
(6,5)
HiPco
(9,4)
(8,6)
(7,5)
(7,6)
(8,4)
(6,5)
Excitation wavelength (nm)
Emission wavelength (nm)
850
800
750
700
650
600
550
500
900
1000
1100
1200
1300
1400
4500
4000
3500
3000
2500
2000
1500
1000
500

Graphic Abstract

Diameter Controlled CVD Synthesis of Single-Walled Carbon Nanotubes
Theerapol THURAKITSEREE, Erik EINARSSON, Rong XIANG, Pei ZHAO, Shinya AIKAWA, Shohei CHIASHI, Junichiro SHIOMI, and Shigeo MARUYAMAs

We systematically investigated the influence of catalyst preparation conditions on the mean diameter of SWNTs synthesized by the alcohol catalytic chemical vapor deposition (ACCVD) process. We successfully reduced the average diameter of the SWNTs by modifying the catalyst preparation, most drastically by water-assisted reduction prior to ACCVD. We also report the use of Co/Rh as a new binary catalyst system for SWNT synthesis.